High-loading Ga-exchanged MFI zeolites as selective and coke-resistant catalysts for nonoxidative ethane dehydrogenation

Mengwen Huang[a], Shunsaku Yasumura[a], Lingcong Li[a], Takashi Toyao[a,b], Zen Maeno*[,a], Ken-ichi Shimizu*[,a,b]

a Institute for Catalysis, Hokkaido University, N-21, W-10, Sapporo 001-0021, Japan

b Elements Strategy Initiative for Catalysts and Batteries, Kyoto University, Katsura, Kyoto 615-8520, Japan

*Corresponding authors

Zen Maeno, E-mail: maeno@cat.hokudai.ac.jp

Ken-ichi Shimizu, E-mail: kshimizu@cat.hokudai.ac.jp

† Electronic supplementary information (ESI) available.

ABSTRACT: In this paper, we investigated the effects of Ga loading amount and H_2 treatment temperature for reductive solid-state ion-exchange reaction on the generated Ga species in Ga-exchanged MFI zeolites (Ga-MFIs) as well as their catalysis for ethane dehydrogenation (EDH). For the formation of isolated Ga hydrides in zeolites, $[GaH]^{2+}$ ions were preferentially formed in the low-loading Ga-MFI (Ga/Al = 0.3) treated with H_2 at 550 ˚C, corresponding to the conventional preparation conditions, (Ga-MFI-0.3(550)), while the high Ga loading (Ga/Al = 1.0) and high-temperature H_2 treatment (800 ˚C) (Ga-MFI-1.0(800)) induced the formation of $[GaH_2]^+$ ions as the major Ga hydrides, as revealed by *in situ* Fourier-transform infrared spectroscopy including the isotope experiment using D_2 instead of H_2. In the context of other Ga species, such as Ga^+ cations and partially reduced Ga oxides (GaO_X), Ga^+ cations and GaO_x coexist in Ga-MFI-0.3(550), as indicated by pyridine adsorption experiments. On the other hand, GaO_x was hardly observed and the larger amount of Ga^+ cations was formed in Ga-MFI-1.0(800). The remaining Brønsted acid sites (BASs) were also characterized by NH_3 adsorption experiment. In the non-oxidative C_2H_6 dehydrogenation, Ga-MFI-1.0(800) exhibited high selectivity owing to low coke formation, resulting in the highest durability among a series of Ga-MFIs tested. Under the optimized conditions, Ga-MFI-1.0(800) exhibited the highest C_2H_4 formation rate among the previously reported Pt-free catalysts. Based on the combined results of characterizations, catalyst tests, and kinetic studies, the high selectivity and durability of Ga-MFI-1.0(800) can be ascribed to the low amount of the remaining BASs by isolated Ga species ($[GaH]^{2+}$, $[GaH_2]^+$ ions and Ga^+ cations) as well as the major formation of $[GaH_2]^+$ ions among isolated Ga hydrides.

1. Introduction

Hydrides in/on solid materials have garnered increasing attention and interest in various research fields.[1–8] In the field of catalysis, isolated metal hydrides on solid supports have been recognized as key species for hydrogenation and dehydrogenation reactions using heterogeneous catalysts since the 1970s.[7,8] On metals[10–16] and metal oxides[17–25], H_2 is cleaved in a homolytic or heterolytic manner to form metal–hydrogen (M−H) bonds. However, their analysis is difficult owing to the complexity of the surface structures of metals/metal oxides, as well as the instability of generated hydride species. In addition, the elucidation of their catalysis is complicated because metal hydrides are often formed as transient species during catalytic reactions. To design well-defined metal hydrides, an alternative method that utilizes surface organometallic chemistry has been explored.[26–29] Although various transition metal hydrides were successfully synthesized, they were thermally decomposed under high-temperature conditions, thus limiting their catalytic applications. The study of the formation and catalysis of surface metal hydrides under high-temperature conditions is still a formidable task.

Ga-loaded zeolites, such as Ga-exchanged MFI (Ga-MFI), have been utilized as promising catalysts for light alkane transformations.[30–32] Ga-MFI is typically prepared by immobilization of Ga_2O_3 on MFI via impregnation of $Ga(NO_3)_3$ and calcination, followed by H_2 treatment to promote reductive solid-state ion-exchange (RSSIE) reactions. Various types of Ga species, including those reduced (Ga^+ cations and isolated Ga hydrides) and those oxidized (Ga oxides, $[GaO]^+$, and $[Ga(OH)_2]^+$), are possibly formed and proposed as active sites for the dehydrogenation of light alkanes and several reaction mechanisms are proposed. [33–38] Alkane dehydrogenation on Ga oxides has been explored regardless of differences in structure and supports [39–46]; however, Ga-oxide-based catalysts often suffer from quick deactivation. Under reductive conditions without any oxidant, Ga hydrides are considered to be

more active sites than Ga^+ cations. The presence of Ga hydrides was first proposed by Iglesia based on *in situ* X-ray absorption spectroscopy (XAS) measurement of Ga-MFI with Ga/Al = ca. 0.3 under H_2 flow at around 500 °C.[47] Kazansky et al. revealed the structure of Ga hydrides formed in the H_2 treated Ga-MFI with Ga/Al = 1.0 using *in situ* infrared (IR) spectroscopy, where $[GaH]^{2+}$ and $[GaH_2]^+$ ions were identified and the proportion of $[GaH_2]^+$ increased by increasing the treatment temperature from 300 to 500 °C.[48] However, the detailed Ga speciation, including remaining Ga-oxides, and the dehydrogenation catalysis have not been extensively investigated. The effects of Ga/Al (0−1.7) and Si/Al ratios on the formation of Ga species were determined by Xu et al. where the partially reduced Ga oxide (GaO_X) oligomers/aggregation remained for high Ga loading (Ga/Al > 0.45) after H_2 treatment at 500 °C.[49]. Bell et al. prepared Ga-MFI containing only Ga species via the vapor-phase ion-exchange reaction of H-MFI with $GaCl_3$ (Ga/Al = 0.05−0.6) followed by H_2 treatment at 550 °C. $[GaH]^{2+}$ ions were mainly formed in the Ga-MFI with a low Ga/Al ratio of 0.2, and an increase in Ga/Al above 0.5, affording a mixture of $[GaH]^{2+}$ and $[GaH_2]^+$ ions.[50] $[GaH]^{2+}$ ions are more active species than $[GaH_2]^+$ ions for C_3H_8 dehydrogenation (PDH) although $[GaH_2]^+$ and $[GaH]^{2+}$ ions exhibited similar activities in C_2H_6 dehydrogenation (EDH).[51,52] Lercher et al. investigated the Ga/Al dependency (Ga/Al = 0−1.5) of the reaction rate for PDH and compared it with that of the amounts of Ga^+, Brønsted acid sites (BASs), and GaO_X oligomers. The medium loading Ga-MFI with Ga/Al = 0.5 exhibited the highest reaction rate. The pair of Ga cations and BASs is proposed as the active site for PDH, where $[GaH]^{2+}$ ions are formed from the Ga^+ cations-BASs pairs and thereafter activate C_3H_8.[53] The similar conclusion was proposed by Xu et al.[54] The formation of active Ga hydrides ($[GaH]^{2+}$ ions and H^+-$[GaH_2]^+$ pair) from Ga^+ cations with BASs under reductive conditions was also discussed by Bell et al. [51,52] Aforementioned studies have mainly focused on the characterization and dehydrogenation catalysis of low- to medium-loading Ga-MFIs [33,34,47,50–53] and the reports on the Ga-MFIs with high Ga loading (Ga/Al = ca. 1.0) have been limited. [48,49] The dehydrogenation catalysis of high-loading Ga-MFIs have been rarely explored.[38]

We have recently reported the formation of isolated In-hydrides in the form of $[InH_2]^+$ by high-temperature H_2 treatment of In-exchanged CHA zeolite (In-CHA) prepared via the RSSIE reaction. In-CHA exhibited high selectivity owing to low coke formation and good durability for EDH, where $[InH_2]^+$ ions serve as the catalytically active sites rather than In^+ cations and $[InH]^{2+}$ ions.[55] In contrast, Ga-CHA exhibited low selectivity and durability owing to severe coke formation, although the apparent activation barrier for dehydrogenation is much lower than that for In-CHA. The high selectivity of In-CHA can be interpreted as the formation of $[InH_2]^+$ ions rather than $[InH]^{2+}$ ions based on transition state (TS) calculations. Our calculation results demonstrate that the *in situ* generated BASs are relatively stable during the EDH on $[InH]^{2+}$ ions, whereas the reaction on $[InH_2]^+$ ions does not involve the *in situ* generation of BASs as stable intermediates. The abundance of *in situ* generated BASs for $[InH_2]^+$ ions is likely less than that of $[InH]^{2+}$ ions, resulting in the low coke formation in the In-CHA-catalyzed EDH. A similar difference in the reaction mechanisms between $[GaH]^{2+}$ and $[GaH_2]^+$ ions is also indicated by the comparison of the TS calculation for EDH by Ga-MFI in a recent paper by Bell et al.[56] These mechanistic insights imply that controlling the formation of $[GaH]^{2+}$ and $[GaH_2]^+$ ions influences the catalytic performance of Ga-zeolites for EDH.

In this paper, we aimed at investigating the effects of Ga loading amount and H_2 treatment temperature on the Ga species, including isolated Ga hydrides, in Ga-MFIs as well as their catalysis in EDH. $[GaH]^{2+}$ ions were preferentially formed in the low-loading Ga-MFI (Ga/Al = 0.3) treated with H_2 at a conventional temperature of 550 °C (Ga-MFI-0.3(550)), whereas the high-loading Ga-MFI (Ga/Al = 1.0) treated at a high temperature of 800 °C (Ga-MFI-1.0(800)) afforded $[GaH_2]^+$ ions as the major Ga hydrides. It is also found that the high temperature H_2 treatment of 800 °C was required to extensively promote the RSSIE for high-loading Ga-MFIs and that the different H_2 treatment temperature affects the proportion of $[GaH]^{2+}$ and $[GaH_2]^+$ ions in high-loading Ga-MFIs. In EDH, Ga-MFI-1.0(800) exhibited higher selectivity owing to much less coke formation compared to low-loading and medium-loading Ga-MFIs. We also discussed the difference between Ga-MFI-0.3(550) and 1.0(800) in *in situ* XAS measurements and kinetic study as well as the influence of different proportion of $[GaH]^{2+}$ and $[GaH_2]^+$ ions in the EDH catalyzed by high-loading Ga-MFIs.

2. Methods

2.1. Catalyst preparation

The Ga-exchanged MFI zeolite catalysts were synthesized by the reductive solid-state ion-exchange method (RSSIE). First, a 1g NH_4^+-type MFI (SiO_2/Al_2O_3 = 22.3, Tosoh) was mixed with $Ga(NO)_3{\cdot}nH_2O$ (n = 7-9, Wako) in 50 mL of deionized water. The water was removed from the mixture by the rotary evaporator under vacuum conditions. The resulting solid was dried in an oven and then calcined under air flow at 500 °C for 1 h to give the Ga_2O_3-modified MFI zeolite. After that, the Ga_2O_3-modified MFI zeolite was treated under 10% H_2/He flow at different temperature for 30 min, affording Ga-MFI-X(Y) where X and Y denotes the Ga/Al ratio and H_2 treatment temperature. The Ga/Al value was determined on the basis of the amounts of $Ga(NO_3)_3{\cdot}nH_2O$ and MFI zeolite.

2.2. *In situ* FTIR measurement

In situ FTIR spectroscopy studies were carried out using a JASCO FT/IR-4600 spectrometer with a mercury cadmium telluride (MCT) detector and a flow-type quartz IR cell connected to a flow system. For characterization of Ga hydrides, the background spectrum was taken under 50 °C without catalyst in He atmosphere. The IR pellet of Ga-MFI-X(Y) was *in situ* obtained through the preparation of self-supported pellet of the corresponding Ga_2O_3-modified zeolite (Ga/Al = 0.3, 0.5, and 1.0) and set into the IR cell followed by H_2 treatment at different temperature (10% H_2/He flow at 550, 700 and 800 °C). Note that the same amount (40 mg) of Ga-MFIs was used for these IR experiments regardless of different Ga loading amount. The temperature was decreased to 50 °C under a H_2/He flow and the FTIR spectrum was recorded without exposure to air. After that, the sample was treated under He flow at 800 °C to decompose Ga hydrides and then the IR spectrum was recorded again at 50 °C. Subtracting the IR spectrum after He treatment from the one before He treatment afforded the difference spectrum showing the peak derived from Ga hydrides. For pyridine (Py) adsorption experiments, the IR pellet was made *in situ* in the same manner as described above and cooled down to 150 °C in H_2/He atmosphere. Subsequently, purging with He to remove the H_2 and taking the background spectrum. Py was repeatedly introduced until the intensity of the bands derived from adsorbed Py species reached its saturation and then purged with He, followed by obtaining the IR spectra for adsorbed Py species. For NH_3 adsorption experiments, after the *in situ* preparation of IR pellet of Ga-MFI-X(Y), temperature was decreased to 50 °C under H_2/He flow and then purging by He to remove H_2. Prior to the NH_3 adsorption (10% NH_3/He), the background spectra were obtained under He flow at 50 °C. The IR spectra were obtained after the saturation of the peak area for adsorbed NH_3 and purging with He for 15 min.

2.3. *In situ* XAS measurement

A Ga K-edge XAS measurement was conducted in transmission mode in the BL14B2 station attached to a Si(311) monochromator at SPring-8 (JASRI), Japan (Proposal No. 2020A1695). The self-supported disk of a Ga_2O_3-modified MFI (Ga/Al = 0.3 or 1.0) was prepared and then put in a flow-type quartz cell with a flow reaction system was used. The XAS spectra were continuously recorded during the RSSIE reaction under 10% H_2/He flow with increasing the temperature from 200 to 550 or 800 °C. Note that the same amount (80 mg) of Ga-MFIs was used for these IR experiments regardless of different Ga loading amount. The absorption edge (E_0) was defined as the 1st inflection point.

2.4. EDH reactions

The catalyst test of C_2H_6 dehydrogenation over Ga-MFI-X(Y) was carried out at 660 °C in flow type reactor under atmospheric pressure conditions. Prior to the reaction, the corresponding Ga_2O_3-modified MFI catalyst with the loading of 0.1 g was pretreated with 10% H_2/He (10 mL/min) at different temperature for 30 min. After purging with He to remove H_2, the gas reactant (10 mL/min of 10% C_2H_6/He) was introduced to the flow type system at 660 °C. The conversion, selectivity, and carbon balance were determined by gas chromatography (GC) analysis which conducted by using Shimadzu GC-14B with a flame ionization detector (FID) and a Unipack S column. The details for determination were described in ESI†.

2.5. TPO measurement

TPO measurement was performed using BELCAT II (MicrotracBEL). 40 mg of the Ga-MFI-X(Y) after 2 h reaction was used for the TPO experiment. First, the sample was pretreated at 150 °C for 30 min under He atmosphere. Then switching the gas flow to 2% O_2/He (40 mL/min) and subsequently increasing the temperature to 800 °C at 5 °C/min. During the measurement, the CO_2 generated through coke oxidation (m/z = 44) was monitored by mass spectroscopy (BELmass, MicrotracBEL).

3. Results and Discussion

3.1. Characterization of Ga species by *in situ* FTIR spectroscopy

In situ FTIR spectroscopy of a series of Ga-MFI was performed to examine the different Ga hydrides in MFI zeolites. In the previous literature, Ga-MFI was prepared conventionally under low to medium Ga loading (Ga/Al = 0.3−0.5) and H_2 treatment at around 500−600 °C, and two types of Ga hydrides are formed: $[GaH]^{2+}$ and $[GaH_2]^+$ ions.[48] The Ga hydrides exhibit peaks assignable to Ga−H stretching vibrations at around 2060 and 2040 cm^{-1}, respectively.[48,50] A recent theoretical study supports these peak assignments and shows that isolated Ga hydrides is kinetically trapped at high temperatures despite the thermodynamically favored formation of Ga^+ cations [56] although these vibration frequencies are higher than those reported in inorganic Ga hydride complexes.[57,58] Even though a few reports on Ga speciation for Ga-MFI with high Ga loading amount have appeared,[48,49,53] a high-loading Ga-MFI treated with H_2 at higher temperatures has been rarely investigated.

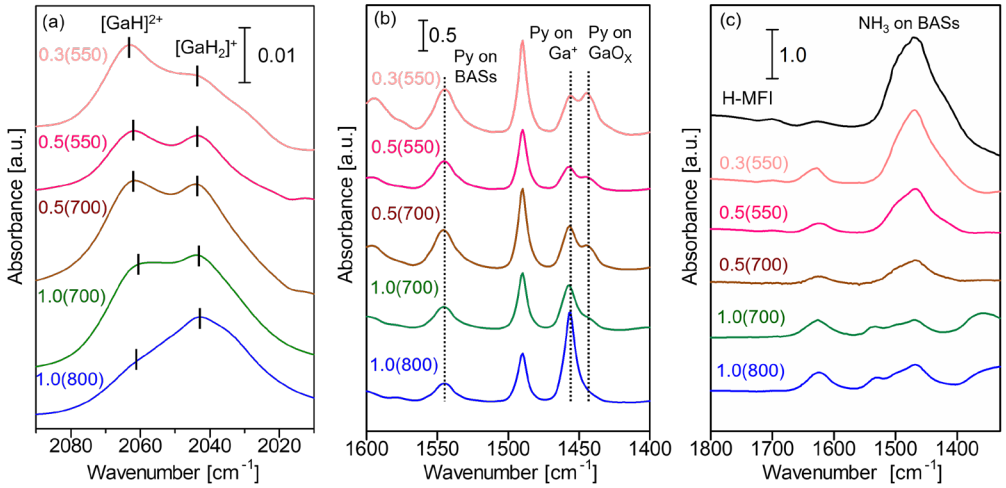

Fig. 1. Characterization of Ga species in Ga-MFI-X(Y) (X: Ga/Al ratio, Y: H_2 treatment temperature). (a) Difference IR spectra obtained at 50 °C without exposure to air. (b) IR spectra of adsorbed pyridine (Py) species at 150 °C. (c) IR spectra of adsorbed NH_3 species at 50 °C. The same amount (40 mg) of Ga-MFIs was used for these IR experiments regardless of different Ga loading amount. For (a), the IR spectrum after H_2 treatment at different temperature was recorded at 50 °C and then the sample was further treated at 800 °C under He flow followed by cooling to 50 °C to record the spectrum. The difference IR spectra were obtained by subtracting the spectra after He treatment from the ones after H_2 treatment. For (b) and (c), the spectra were recorded after the saturation of Py or NH_3 adsorption followed by He purge. Prior to the adsorption experiment, the background spectra were taken under He flow.

The IR spectra were recorded at 50 °C after H_2 treatment for 1 h at different temperatures. Afterwards, the sample was treated under He at 800 °C for 1 h and subsequently cooled to 50 °C again to obtain the spectra. The difference spectrum was obtained by subtracting the spectra taken after He treatment from those taken after H_2/He treatment for each sample (**Fig. 1a**, the wide-range spectra are shown in **Fig. S1** in ESI†). The IR spectrum for Ga-MFI-0.3(550) exhibited a stronger band at 2063 cm^{-1} derived from $[GaH]^{2+}$ ions with a weaker band at 2043 cm^{-1} derived from $[GaH_2]^+$ ions. For Ga-MFI-0.5(550), both bands were clearly observed, where the band intensity derived from $[GaH_2]^+$ ions is similar to that of $[GaH]^{2+}$ ions. The increase in the H_2 treatment temperature from 550 to 700 °C increased both bands in intensity, indicating that the amount of both Ga hydrides were increased. When Ga/Al ratio was increased from 0.5 to 1.0 (Ga-MFI-1.0(700)), the band for $[GaH_2]^+$ ions became higher in intensity than that for $[GaH]^{2+}$ ions. Upon further increasing the H_2 treatment temperature from 700 to 800 °C (Ga-MFI-1.0(800)), the band intensity for $[GaH]^{2+}$ ions decreased, and the band derived from $[GaH_2]^+$ ions was mainly observed. In a separate experiment, Ga hydrides were regenerated by H_2 treatment of the He-treated Ga-MFI-1.0(800) (See **Fig. S2** in ESI†), confirming the decomposition of Ga hydrides by high-temperature He treatment (800 °C) and the formation of Ga hydrides by high-temperature H_2 treatment (800 °C). To further support the formation of Ga hydrides, the exchange reaction with D_2 was performed for Ga-MFI-1.0(800). The main band derived from $[GaD_2]^+$ ions and the minor band assignable to $[GaD]^{2+}$ ions appeared around 1460 and 1470 cm^{-1}, respectively, with the negative bands for $[GaH_2]^+$ and $[GaH]^{2+}$ ions observed at 2043 cm^{-1} and 2063 cm^{-1}. (**Fig. S3** in ESI†), supporting the formation of $[GaH]^{2+}$ and $[GaH_2]^+$ ions by high temperature H_2 treatment. The XRD measurements of a series of Ga-MFIs revealed that the diffraction pattern of MFI zeolites was maintained (**Fig. S4** in ESI†), which confirmed the preservation of zeolite frameworks after RSSIE reactions.

Pyridine (Py) adsorption experiments were conducted to investigate other Ga species. BASs, Ga^+ cations, and GaO_X can be identified by the difference in frequencies derived from adsorbed Py species.[49,53] Lercehr et al. extensively performed the pyridine adsorption experiments for Ga speciation in Ga-MFIs with a wide-range of Ga/Al (0−1.5) prepared by H_2 treatment at 600 ˚C. In their system, partially reduced Ga oxide (GaO_X) oligomers/aggregation remained for high Ga loading (Ga/Al ≥ 0.5).[53] Xu et al. reported the FTIR spectroscopic study for Ga-MFIs with a wider-range of Ga/Al (0−1.7). The temperature of H_2 treatment for reductive solid-state ion-exchange (RSSIE) reaction was limited to 500 ˚C and GaO_X remained for high Ga loading (Ga/Al > 0.45).[49] The sample was prepared *in situ* under H_2/He flow in the same manner as described above and cooled to 150 °C under H_2/He flow. After taking the background spectra under He flow, Py was repeatedly introduced until the intensity of the bands for adsorbed Py species reached saturation and thereafter purged with He, followed by recording the IR spectra. The spectrum for Ga-MFI-0.3(550) (**Fig. 1b**) exhibited three peaks derived from Py on BASs, Ga^+ cations, and GaO_X at 1555, 1457, and 1446 cm^{-1}, respectively.[53] Note that other adsorbed Py species on strong Lewis acid sites, such as Al^{3+} cations, or defect sites of zeolites also possibly contribute to the

absorption bands.[53] For Ga-MFI-0.5, the higher temperature treatment resulted in higher peak intensities for Ga^+ cations and GaO_X, indicating that the reduction of Ga_2O_3 was facilitated. When the Ga/Al ratio was increased to 1.0 (Ga-MFI-1.0(700)), the peak intensity for Ga^+ cations increased with the decrease of other peaks for BASs and GaO_X. A further increase in the H_2 treatment temperature to 800 °C afforded the highest peak intensity for Ga^+, although the peak derived from GaO_X was scarcely observed, indicating that the RSSIE reaction almost completely occurred.

Furthermore, NH_3 adsorption experiments were conducted to quantify the amount of the remaining BASs. The *in situ* prepared samples were exposed to 10% NH_3/He flow at 50 °C until the saturation of the peak area for the adsorbed NH_3 on the BASs (NH_4^+)[59] at around 1450 cm^{-1} and then purged with He for at least 15 min. Prior to NH_3 adsorption, background spectra were obtained under He flow at the same temperature. The amount of the remaining BASs was normalized by the peak area for NH_4^+ in H-MFI, prepared by He treatment of NH_4-MFI at 700 °C. The IR spectra for NH_3-adsorbed Ga-MFI-0.3(550) exhibited a moderate peak for NH_4^+, where the normalized area (denoted as $H^+/H^+_{H\text{-}MFI}$) was calculated to be 70% (**Fig. 1c**). Considering the formation of $[GaH]^{2+}$ ions that are charge-compensated by paired Al sites and the presence of remaining GaO_X, the RSSIE reaction was incomplete. For Ga-MFI-0.5, the $H^+/H^+_{H\text{-}MFI}$ value decreased from 38% to 18% with an increase in the H_2 treatment temperature from 550 to 700 °C. When Ga/Al was increased to 1.0, $H^+/H^+_{H\text{-}MFI}$ was low (12% and 18% at 700 °C and 800 °C, respectively). The higher $H^+/H^+_{H\text{-}MFI}$ value for Ga-MFI-1.0(800) than (700) is ascribed to the higher proportion of $[GaH_2]^+$ ions that require one Al sites.

From the above results, the speciation of Ga species in Ga-MFI prepared under different Ga/Al ratios and H_2 treatment temperatures is summarized as follows. $[GaH]^{2+}$ ions were preferentially formed in the low Ga loading (Ga/Al = 0.3), whereas the middle Ga loading (Ga/Al = 0.5) resulted in the moderate formation of both $[GaH]^{2+}$ and $[GaH_2]^+$ ions. In the high-loading Ga-MFI (Ga/Al = 1.0) treated with H_2 at a high temperature of 800 °C, the proportion of $[GaH_2]^+$ ions was the highest. In addition, the RSSIE reaction almost completely occurred, leading to the predominant formation of $[GaH_2]^+$ ions and Ga^+ cations as Ga hydrides and other Ga species, respectively. This result can be ascribed to the preferential formation of monovalent Ga species ($[GaH_2]^+$ ions and Ga^+ cations) rather than divalent Ga species ($[GaH]^{2+}$ ions) under high Ga loading conditions above Ga/Al = 0.5.

3.2. *In situ* XAS measurements for Ga-MFI-0.3(550) and 1.0(800)

Iglesia et al. proposed the formation of Ga hydrides in Ga-MFI based on the lower energy shift in the XANES spectrum and the disappearance of EXAFS features[47] while Hensen et al. attributed the shift to the formation of Ga^+ cations.[60] Wilkinson reported the XAS spectra for Ga^+ cations supported on β''-Al_2O_3 or in $GaZr_2(PO_4)_3$, where their absorption edge energies were much lower than that for Ga^{3+} in $ZnGa_2O_4$.[61] Hock et al. recently performed the synthesis and XAS measurements of several organometallic model Ga complexes and concluded that the lower energy shift is equally interpreted as the formation of Ga^+ cations and Ga hydrides.[62]

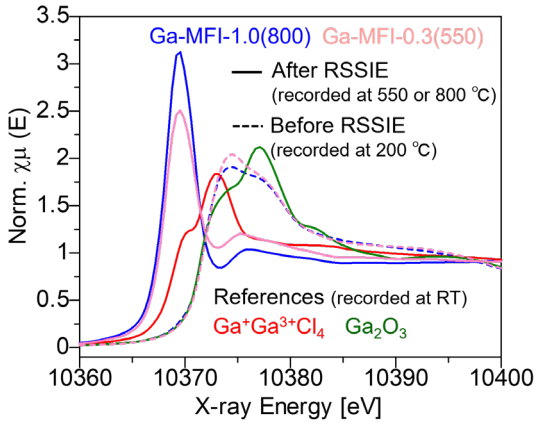

Fig. 2. *In situ* Ga K-edge XAS spectra of Ga-MFI-0.3(550) and 1.0(800) (pink and blue lines, respectively) before and after RSSIE (dot and solid lines, respectively). The spectra before RSSIE were obtained at 200 ˚C whereas the ones after RSSIE were recorded at the same temperature as H_2 treatment. For references (Ga_2O_3, $Ga^+Ga^{3+}Cl_4$), the spectra were obtained at room temperature.

In this work, *in situ* XAS measurements of Ga-MFI-0.3(550) and 1.0(800) were conducted and then the obtained spectra were compared. The self-supported disk of the corresponding Ga_2O_3-modified MFI zeolite after calcination was exposed to a 10% H_2/He flow at 200 °C and thereafter heated to 550 or 800 °C in a quartz cell to promote RSSIE reactions, as mentioned above. During the H_2 treatment, the XAS spectra were continuously recorded until the spectrum remained unchanged. The absorption edge of the XANES spectrum of Ga-MFI-0.3(550) and 1.0(800) before RSSIE was quite similar to that of bulk Ga_2O_3 (**Fig. 2**, E_0 = 10372.0,

10371.8, and 10371.6 eV, respectively. E_0 denotes the energy of the absorption edge, defined as the first inflection point). Note that the XAS measurements of Ga-MFIs before RSSIE were performed at 200 °C while the XAS spectra of reference samples were obtained at room temperature.

After the H_2 treatment at each temperature, the XAS spectra were recorded without exposure to air at the same temperatures (550 or 800 °C). The absorption edge shifted to a lower value in the energy in both cases (E_0 = 10368.1 and 10368.3 eV for Ga-MFI-0.3(550) and 1.0(800), respectively), which are almost the same as that of Ga^+ in $Ga^+Ga^{3+}Cl_4$ (E_0 = 10369.3 eV)[53,62] (**Fig. 2**). However, the intensity of the peak around 10370 eV is much higher for Ga-MFI-1.0(800) than Ga-MFI-0.3(550). The stronger peak for Ga-MFI-1.0(800) is ascribed to the occurrence of sufficient RSSIE reaction and the exclusive formation of isolated Ga species ($[GaH]^{2+}$ and $[GaH_2]^+$ ions as well as Ga^+ cations), which is consistent with the FTIR results as discussed above.

3.3. EDH reaction using Ga-MFI-X(Y)

Next, the catalysis of a series of Ga-MFIs was compared in EDH reaction. This transformation is promising for obtaining C_2H_4, which is one of the most important bulk chemicals in industries, because of the increasing availability of cheap C_2H_6 from shale gas.[63–65] In comparison with the oxidative EDH, the high selectivity for C_2H_4 is obtained owing to the absence of an oxidant. Cracking reactions without catalysts are commercially operated, but severe reaction conditions above 1000 °C are required. In addition, rapid cooling of the outlet gas is necessary below 800 °C to suppress the successive reaction of C_2H_4. To decrease the reaction temperature, catalytic EDH has been investigated using mainly Pt-based alloys, Cr, and Ga catalysts.[63–65] However, most catalysts are easily deactivated owing to coke formation. In the context of EDH using Ga-MFI, the Ga-MFI with low-to-medium Ga/Al values have been studied previously[39,52], but the dehydrogenation catalysis of high-loading Ga-MFI has been rarely investigated.

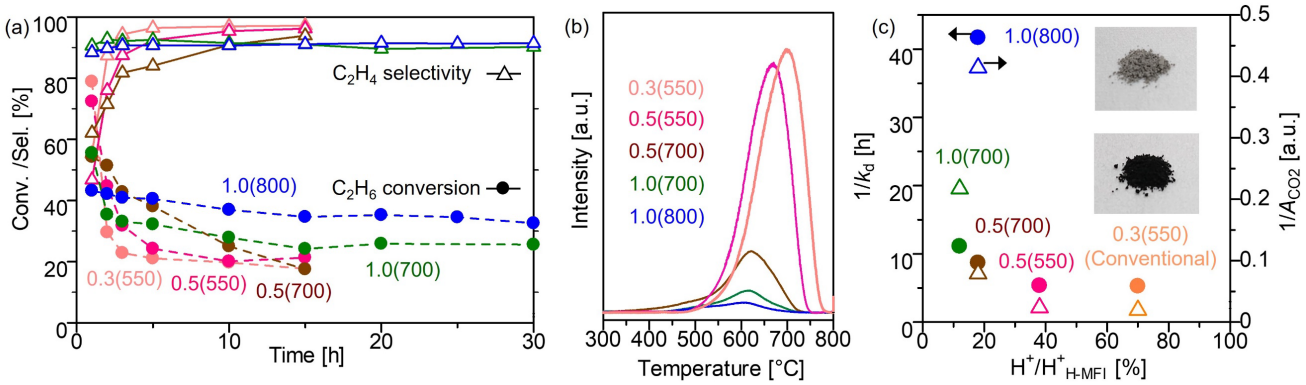

Fig. 3. (a) Conversion and selectivity in EDH using different Ga-MFI-X(Y). Reaction conditions: 100 mg of Ga-MFI-X(Y), 10 mL/min of 10% C_2H_6/He, and 660 °C. (b) TPO profiles of a series of Ga-MFI after reaction for 2 h. (c) Plots of reciprocals of k_d in dehydrogenation tests and A_{CO2} in TPO experiments (indexes of durability and coking suppression, respectively) as a function of relative amount of the remaining BASs based ($H^+/H^+_{H\text{-}MFI}$). Upper and lower inset pictures are the Ga-MFI-1.0(800) and 0.3(550) after reactions for 2 h, respectively.

Table 1. Conversion, selectivity, and carbon balance values at 1, 15, and 30 h in EDH catalyzed by Ga-MFI-X(Y)[a]

Catalyst	Time [h]	Conv. [%][b]	Sel. [%][b]	Carbon balance [%][b]	k_d [h^{-1}][c]
GaMFI-0.3(550)	1	79	55	34	0.190
	15	18	97	96	
GaMFI-0.5(550)	1	72	47	52	0.187
	15	21	96	100	
GaMFI-0.5(700)	1	54	62	62	0.115
	15	18	94	97	
GaMFI-1.0(700)	1	56	91	61	0.090

	15	26	91	99	
	30	25	90	97	
GaMFI-1.0(800)	1	43	89	85	0.024
	15	35	91	99	
	30	33	91	98	

[a]Reaction conditions: 100 mg of Ga-MFI-X(Y), 10 mL/min of 10% C_2H_6/He, and 660 °C. [b]Determined by GC-FID. More information is presented in SI. [c]Deactivation rate for 15 h of reaction. The determination is described in SI.

The EDH using Ga-MFI-X(Y) was carried out at 660 °C (**Fig. 3a** and **Table 1**). Ga-MFI-0.3(550), prepared under conventional conditions, exhibited a high initial conversion (78%), but the selectivity for C_2H_4 was quite low (55%) at 1 h. The conversion of Ga-MFI-0.3(550) immediately decreased to about 20% within 3 h. Ga-MFI-0.5(550) also exhibited a similar initial conversion and selectivity (72% and 47%, respectively), whereas the conversion decreased to 22% after 8 h. Increasing the H_2 treatment temperature from 550 to 700 °C (Ga-MFI-0.5(700)) improved the C_2H_4 selectivity to 62% with a slight decrease in the initial conversion to 55%, leading to slightly better durability. When Ga/Al was increased from 0.5 to 1.0, the C_2H_4 selectivity was significantly enhanced, reaching about 90%. Although the initial conversion of Ga-MFI-1.0(800) (43%) was lower than that of Ga-MFI-1.0(700) (55%), the durability of Ga-MFI-1.0(800) was much better. The conversion of Ga-MFI-1.0(800) after 30 h of reaction was still higher than 30%, whereas that for Ga-MFI-1.0(700) decreased to less than 30% at 10 h. The deactivation rate (k_d)[65] for the 15 h reaction was calculated and thereafter compared among a series of Ga-MFIs. The k_d value increased in the order of Ga-MFI-1.0(800) < 1.0(700) < 0.5(700) < 0.5(550) < 0.3(550), indicating that Ga-MFI-1.0(800) exhibited the highest durability. Under the optimized reaction conditions using Ga-MFI-1.0(800), the C_2H_4 formation rate reached 72.1 mmol/(g·h) with good conversion and selectivity values (28.5% and 92.6%, respectively) as well as a low deactivation rate (0.014 h^{-1}) (**Fig. 4**). This formation rate is the highest among the reported Pt-free catalysts (**Table S1** in in ESI†)[55,66,75,67–74]. After the reaction, Ga-MFI-1.0(800) could be regenerated by oxidation treatment (a 5% O_2/He flow at 600 °C for 1.5 h) followed by H_2 treatment at 800 °C. The regenerated catalyst exhibited similar initial conversion and selectivity values to the original values (See **Fig. S5** in ESI†).

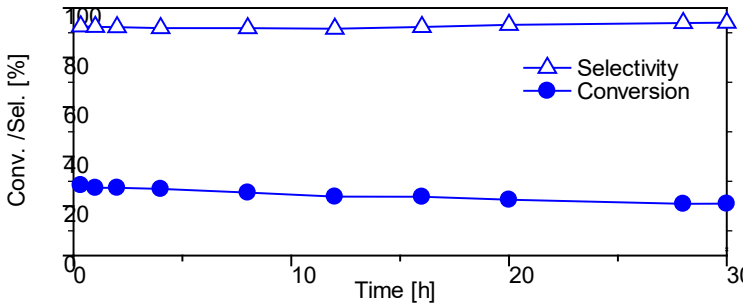

Fig. 4. Ga-MFI-1.0(800)-catalyzed EDH under optimized conditions. Reaction conditions: 50 mg of Ga-MFI-1.0(800), 10 mL/min of 50% C_2H_6/He, and 660 °C.

Temperature-programmed oxidation (TPO) experiments were conducted for the Ga-MFI-X(Y) used for the 2 h reaction. The generated CO_2 by coke oxidation was monitored by mass spectroscopy (m/z = 44), and the corresponding peaks were compared. The peak areas (A_{CO2}) for Ga-MFI-0.3(550) and 0.5(550) were much larger than those for others, and the A_{CO2} for Ga-MFI-1.0(800) was the lowest (**Fig. 3b**). These results demonstrate that coke formation was suppressed by the increase in Ga loading and H_2 treatment temperature. To further discuss the reason for coke formation, the reciprocal of k_d as an index of durability and that of A_{CO2} as an index of coking suppression were plotted as a function of the remaining BASs, $H^+/H^+_{H\text{-}MFI}$ (**Fig. 3c**). The trends of these plots were similar, which clearly shows that coke formation was the main cause of deactivation. This is also supported by a comparison of the color of the used Ga-MFI. The Ga-MFI-0.3(550) changed from white to black owing to coke formation after 2 h of reaction, whereas the most durable Ga-MFI-1.0(800) exhibited a gray color (the inset pictures in **Fig. 3c**). Among the tested Ga-MFI except for Ga-MFI-1.0(800), the $1/A_{CO2}$ value increased with a decrease in $H^+/H^+_{H\text{-}MFI}$, indicating that the remaining BASs induce coke formation. However, the $1/A_{CO2}$ value for Ga-MFI-1.0(800) was much higher than that for Ga-MFI-1.0(700) despite the same Ga loading and a higher $H^+/H^+_{H\text{-}MFI}$ value. The higher proportion of $[GaH_2]^+$ ions among isolated Ga hydrides ($[GaH_2]^+$ and $[GaH]^{2+}$ ions) might be the reason for lower coke formation for Ga-MFI-1.0(800). Although the high-loading Ga-MFIs treated with H_2 at lower

temperature below 600 °C has been studied as proton-poor Ga-MFI for cyclodimerization of propane by Price et al. the characterization of Ga species and BASs as well as their effects on catalysis were not investigated. This study revealed the importance of high-temperature H_2 treatment and the influence of proportion of active Ga hydrides in high-loading Ga-MFIs.

3.4. Feasibility of isolated Ga hydrides as active sites based on kinetic studies

The reaction mechanism for alkane dehydrogenation has been discussed by several research groups.[53,56,76,77,78]. Lercher et al. theoretically investigated the PDH mechanism on the pair of Ga^+ cations and BASs via the formation of $[GaH]^{2+}$ ions and reported the experimental activation enthalpy for PDH as 106 kJ/mol. [53] Bell et al. show in the recent theoretical study for EDH that $[GaH]^{2+}$ and $[GaH_2]^+$ ions are more plausible catalytically active sites than Ga^+ cations and propose the following reaction mechanisms; alkyl or carbeinum mechanism on $[GaH]^{2+}$ ions, and alkyl or concerted mechanism on $[GaH_2]^+$ ions.[56] Alkyl mechanism involves the C_2H_4 formation from a pair of $[GaH(C_2H_5)]^+/H^+$ as a rate determining step (RDS) with a theoretical activation enthalpy (theoretical $\Delta H^{\ddagger}$) of 150 kJ/mol whereas a theoretical $\Delta H^{\ddagger}$ is predicted as 118 kJ/mol for the carbenium mechanism on $[GaH]^{2+}$ ions where both the C−H activation of C_2H_6 into a pair of $[GaH_2]^+/C_2H_5^+$ and the formation of C_2H_4 and H_2 from $[GaH_2]^+/C_2H_5^+$ are possibly RDSs. For $[GaH_2]^+$ ions, the alkyl mechanism involves C−H activation of C_2H_6 as an RDS with the theoretical $\Delta H^{\ddagger}$ of 115 kJ/mol, and the concerted mechanism does not compete with the alkyl mechanism owing to a high free energy barrier. These distinctions in reaction mechanisms imply that EDH reactions over $[GaH]^{2+}$ and $[GaH_2]^+$ ions show different kinetics. The same group also reported that $[GaH]^{2+}$ and $[GaH_2]^+$ ions exhibited similar activity for EDH using Ga-MFI with a different loading amount (Ga/Al = 0.05-0.6) where $[GaH]^{2+}$ ions and $[GaH_2]^+$-BAS cation pairs are formed from Ga cations.[51] However, the kinetic study was performed for only the medium-loading Ga-MFI (Ga/Al = 0.5) possessing both $[GaH]^{2+}$ and $[GaH_2]^+$ ions, and they discussed the kinetics for EDH over $[GaH_2]^+$ ions.

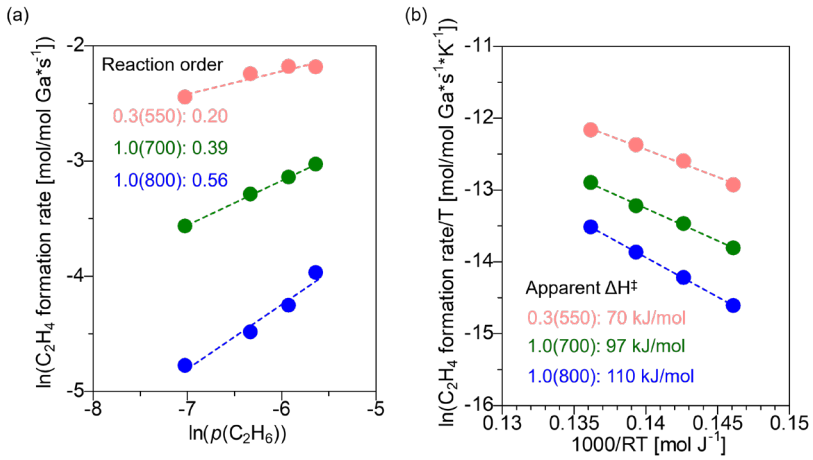

Fig. 5. Kinetic studies using Ga-MFI-0.5(550), 1.0(800), and 1.0(700). C_2H_4 formation rate dependence on (a) $p(C_2H_6)$ and (b) reaction temperature. Reaction condition for (a): 0.1 g of catalyst, 50 mL/min of 2−8% C_2H_6/He, and 600 °C. Reaction condition for (b): 0.1 g of catalyst, 50 mL/min of 4% C_2H_6/He, and 550−610 °C.

In this study, Ga-MFI-1.0(800) and 0.3(550) were used for kinetic studies as Ga-MFIs with the highest proportion of $[GaH_2]^+$ and $[GaH]^{2+}$ ions among tested catalysts, respectively. In the EDH using Ga-MFI-1.0(800), the increase of C_2H_6 partial pressure ($p(C_2H_6)$) increased the formation rate, and the reaction order was 0.56 (**Fig. 5a**), which suggests that the RDS involves C_2H_6 activation. The apparent $\Delta H^{\ddagger}$ determined experimentally from the temperature dependency of the C_2H_4 formation rate was 110 kJ/mol (**Fig. 5b**), which is similar to that in the experimental study reported by Bell et al. using Ga-MFI.[51] These observations support that $[GaH_2]^+$ ions are the active sites in Ga-MFI-1.0(800). In the case of EDH using Ga-MFI-0.3(550), the reaction order with respect to $p(C_2H_6)$ was determined as 0.20 (**Fig. 5a**), and the apparent $\Delta H^{\ddagger}$ was determined to be 70 kJ/mol (**Fig. 5b**), demonstrating the different kinetics from Ga-MFI-1.0(800). Although the obtained $\Delta H^{\ddagger}$ value was lower than the theoretical values reported by Bell et al., the low reaction order value suggest that $[GaH]^{2+}$ ions is more plausible active sites rather than rather $[GaH_2]^+$ ions. Furthermore, the kinetics of Ga-MFI-1.0(700) was investigated to discuss the influence of different proportion of $[GaH_2]^+/[GaH]^{2+}$ ions. The reaction order of $p(C_2H_6)$ was intermediate (0.39) while the apparent $\Delta H^{\ddagger}$ was determined to be 97 kJ/mol, which indicate that both $[GaH_2]^+$ and $[GaH]^{2+}$ ions contribute to the EDH using Ga-MFI-1.0(700). Based on the previous TS calculations reported by Bell et al.,[56] the EDH reaction over $[GaH]^{2+}$ ions involve the *in situ* formation of BASs and/or carbocations as relatively stable intermediates, which possibly induce the coke formation. In contrast, *in situ* generated BASs after C−H bond cleavage via alkyl mechanism smoothly reacts with the coordinated hydrides with the small free energy barriers in the EDH via alkyl mechanism on $[GaH_2]^+$ ions.

The similar difference in reaction mechanism between $[InH_2]^+$ and $[InH]^{2+}$ was also found in our recent study on EDH using In-exchanged zeolites.[55] It can be considered that the abundance of *in situ* generated BASs and/or carbocations during EDH is lower for $[GaH_2]^+$ ions than for $[GaH]^{2+}$ ions. Combined with our experimental results and prior discussion, $[GaH_2]^+$ ions are likely to act as more selective and coke-resistant active sites compared to $[GaH]^{2+}$ ions in EDH. The high selectivity and durability of Ga-MFI-1.0(800) is ascribed to both the low amount of remaining BASs and the main formation of $[GaH_2]^+$ ions.

4. Conclusion

In summary, we prepared a series of Ga-MFIs with different Ga loading amounts and H_2 treatment temperature and examined the generated Ga species and catalysis for EDH. *In situ* FTIR spectroscopy revealed that $[GaH]^{2+}$ ions were preferentially formed in low-loading Ga-MFI (Ga-MFI-0.3(550)), prepared under conventional conditions, whereas both $[GaH]^{2+}$ and $[GaH_2]^+$ ions were moderately formed in the middle-loading Ga-MFI (Ga/Al = 0.5). In contrast, $[GaH_2]^+$ ions were formed as the major Ga hydride in Ga-MFI-1.0(800). The characterization of other Ga species and BASs indicated that high-temperature H_2 treatment was required to promote the RSSIE sufficiently for high-loading Ga-MFI. In Ga-MFI-1.0(800), monovalent Ga species ($[GaH_2]^+$ ions and Ga^+ cations) are mainly formed. The difference of H_2 treatment temperature between 700 and 800 ˚C also affects the proportion of $[GaH]^{2+}$ and $[GaH_2]^+$ ions in high-loading Ga-MFI. In EDH, Ga-MFI-1.0(800) exhibited high selectivity owing to much less coke formation, resulting in the highest durability. Under the optimized reaction conditions, the highest C_2H_4 formation rate was achieved among the reported Pt-free catalyst systems. The kinetic study revealed that isolated Ga hydrides serve as active sites rather than Ga^+ cations. The main reason for the high catalytic performance of Ga-MFI-1.0(800) is a low amount of the remaining BASs by introducing the high loading amount of isolated Ga species. Based on the comparison of high-loading Ga-MFIs treated with different temperature (700 or 800 ˚C), the different proportion of active Ga hydrides ($[GaH_2]^+$ and $[GaH]^{2+}$ ions) also influences their catalysis in EDH.

Author Contributions

M. H. performed catalyst preparation, characterization, catalytic test, and kinetic study, and wrote the draft. S. Y. conducted *in situ* XAS measurement. L. L. investigated catalytic test including optimization of reaction conditions. T. T. and Z. M. critically revised the manuscript. Z. M. and K. S. designed and supervised the whole project.

Conflicts of interest

There are no conflicts of interest to declare.

Acknowledgement

This study was financially supported by KAKENHI (Grant Nos. No. JP17H01341, JP20H02518, JP20H02775, JP21H00012, and JP21H04626) from the Japan Society for the Promotion of Science (JSPS) and by the Japanese Ministry of Education, Culture, Sports, Science, and Technology (MEXT) within the projects “Integrated Research Consortium on Chemical Sciences (IRCCS)” and “Elements Strategy Initiative to Form Core Research Center” (JPMXP0112101003). This study was also supported by the JST-CREST project JPMJCR17J3 and by ENEOS TONEN GENERAL RESEARCH/DEVELOPMENT ENCOURAGEMENT & SCHOLARSHIP FOUNDATION. The authors sincerely thank the technical division of the Institute for Catalysis (Hokkaido University) for manufacturing experimental equipment as well as the technical staff at the Open Facility of Hokkaido University for their assistance. S.Y. acknowledges Grant-in-Aid for JSPS Fellows (DC2).

References

1 R. Mohtadi and S. I. Orimo, *Nat. Rev. Mater.*, 2016, **2**, 1–16.
2 H. Hosono and M. Kitano, *Chem. Rev.*, 2021, **121**, 3121–3185.
3 S. R. Ovshinsky, M. A. Fetcenko and J. Ross, *Science*, 1993, **260**, 176–181.
4 L. Schlapbach and A. Züttel, *Nature*, 2001, **414**, 353–359.
5 P. Chen, Z. Xiong, J. Luo, J. Lin and K. Lee Tan, *Nature*, 2002, **420**, 302–304.
6 H. Kageyama, K. Hayashi, K. Maeda, J. P. Attfield, Z. Hiroi, J. M. Rondinelli and K. R. Poeppelmeier, *Nat. Commun.*, 2018, **9**, 772.
7 C. Copéret, D. P. Estes, K. Larmier and K. Searles, *Chem. Rev.*, 2016, **116**, 8463–8505.
8 P. Serna and B. C. Gates, *Acc. Chem. Res.*, 2014, **47**, 2612–2620.
9 F. Polo-Garzon, S. Luo, Y. Cheng, K. L. Page, A. J. Ramirez-Cuesta, P. F. Britt and Z. Wu, *ChemSusChem*, 2019, **12**, 93–103.
10 T. Kubota, K. Asakura and Y. Iwasawa, *Catal. Lett.*, 1997, **46**, 141–144.
11 M. K. Oudenhuijzen, J. A. Van Bokhoven, J. T. Miller, D. E. Ramaker and D. C. Koningsberger, *J. Am. Chem. Soc.*, 2005, **127**, 1530–1540.

12 D. Teschner, J. Borsodi, A. Wootsch, Z. Révay, M. Hävecker, A. Knop-Gericke, S. D. Jackson and R. Schlögl, *Science*, 2008, **320**, 86–89.
13 K. I. Shimizu, K. Sugino, K. Sawabe and A. Satsuma, *Chem. - A Eur. J.*, 2009, **15**, 2341–2351.
14 R. Juárez, S. F. Parker, P. Concepción, A. Corma and H. García, *Chem. Sci.*, 2010, **1**, 731–738.
15 R. Ishida, S. Hayashi, S. Yamazoe, K. Kato and T. Tsukuda, *J. Phys. Chem. Lett.*, 2017, **8**, 2368–2372.
16 A. Noujima, T. Mitsudome, T. Mizugaki, K. Jitsukawa and K. Kaneda, *Angew. Chem. Int. Ed.*, 2011, **50**, 2986–2989.
17 H. Hattori, Y. Tanaka and K. Tanabe, *J. Am. Chem. Soc.*, 1976, **98**, 4652–4653.
18 E. N. Gribov, S. Bertarione, D. Scarano, C. Lamberti, G. Spoto and A. Zecchina, *J. Phys. Chem. B*, 2004, **108**, 16174–16186.
19 R. Wischert, P. Laurent, C. Copéret, F. Delbecq and P. Sautet, *J. Am. Chem. Soc.*, 2012, **134**, 14430–14449.
20 Z. Wu, Y. Cheng, F. Tao, L. Daemen, G. S. Foo, L. Nguyen, X. Zhang, A. Beste and A. J. Ramirez-Cuesta, *J. Am. Chem. Soc.*, 2017, **139**, 9721–9727.
21 H. Tsuneoka, K. Teramura, T. Shishido and T. Tanaka, *J. Phys. Chem. C*, 2010, **114**, 8892–8898.
22 J. Kondo, Y. Sakata, K. Domen, K. I. Maruya and T. Onishi, *J. Chem. Soc. Faraday Trans.*, 1990, **86**, 397–401.
23 A. Tsoukalou, A. I. Serykh, E. Willinger, A. Kierzkowska, P. M. Abdala, A. Fedorov and C. R. Müller, *Catal. Today*, , DOI:10.1016/j.cattod.2021.04.010.
24 L. Wang, T. Yan, R. Song, W. Sun, Y. Dong, J. Guo, Z. Zhang, X. Wang and G. A. Ozin, *Angew. Chem. Int. Ed.*, 2019, **58**, 9501–9505.
25 N. J. LiBretto, Y. Xu, A. Quigley, E. Edwards, R. Nargund, J. C. Vega-Vila, R. Caulkins, A. Saxena, R. Gounder, J. Greeley, G. Zhang and J. T. Miller, *Nat. Commun.*, 2021, **12**, 2322.
26 C. Copéret, M. Chabanas, R. Petroff Saint-Arroman and J. M. Basset, *Angew. Chem. Int. Ed.*, 2003, **42**, 156–181.
27 C. Copéret, A. Comas-Vives, M. P. Conley, D. P. Estes, A. Fedorov, V. Mougel, H. Nagae, F. Núnez-Zarur and P. A. Zhizhko, *Chem. Rev.*, 2016, **116**, 323–421.
28 F. Rascón, R. Wischert and C. Copéret, *Chem. Sci.*, 2011, **2**, 1449–1456.
29 T. J. Marks, *Acc. Chem. Res.*, 1992, **25**, 57–65.
30 Y. Ono, *Catal. Rev.*, 1992, **34**, 179–226.
31 N. Y. Chen and T. Y. Yan, *Ind. Eng. Chem. Process Des. Dev.*, 1986, **25**, 151–155.
32 D. Seddon, *Catal. Today*, 1990, **6**, 351–372.
33 B. S. Kwak and W. M. H. Sachtler, *J. Catal.*, 1994, 145, 456–463.
34 A. Biscardi and E. Iglesia, *Catal. Today.*, 1996, **31**, 207–231.
35 G. L. Price and V. Kanazirev, *J. Catal.*, 1990, **126**, 267–278.
36 P. Meriaudeau and C. Naccache, *J. Mol. Catal.*, DOI:10.1016/0304-5102(90)85100-V.
37 G. Buckles, G. J. Hutchings and C. D. Williams, *Catal. Lett.*, 1991, **11**, 89–93.
38 G. L. Price, V. Kanazirev, K. M. Dooley and V. I. Hart, *J. Catal.*, 1998, **173**, 17–27.
39 A. Ausavasukhi and T. Sooknoi, *Catal. Commun.*, 2014, **45**, 63–68.
40 H. Saito, S. Maeda, H. Seki, S. Manabe, Y. Miyamoto, S. Ogo, K. Hashimoto and Y. Sekine, *J. Japan Pet. Inst.*, 2017, **60**, 203–210.
41 K. Searles, G. Siddiqi, O. V. Safonova and C. Copéret, *Chem. Sci.*, 2017, **8**, 2661–2666.
42 K. Nakagawa, M. Okamura, N. Ikenaga, T. Suzuki and T. Kobayashi, *Chem. Commun.*, 1998, **3**, 1025–1026.
43 V. J. Cybulskis, S. U. Pradhan, J. J. Lovón-Quintana, A. S. Hock, B. Hu, G. Zhang, W. N. Delgass, F. H. Ribeiro and J. T. Miller, *Catal. Letters*, 2017, **147**, 1252–1262.
44 Y. Cheng, H. Gong, C. Miao, W. Hua, Y. Yue and Z. Gao, *Catal. Commun.*, 2015, **71**, 42–45.
45 P. Castro-Fernández, D. Mance, C. Liu, I. B. Moroz, P. M. Abdala, E. A. Pidko, C. Copéret, A. Fedorov and C. R. Müller, *ACS Catal.*, 2021, **11**, 907–924.
46 E. A. Uslamin, H. Saito, Y. Sekine, E. J. M. Hensen and N. Kosinov, *Catal. Today*, 2021, **369**, 184–192.
47 G. D. Meitzner, E. Iglesia, J. E. Baumgartner and E. S. Huang, *J. Catal.*, 1993, **140**, 209–225.
48 V. B. Kazansky, I. R. Subbotina, R. A. van Santen and E. J. M. Hensen, *J. Catal.*, 2004, **227**, 263–269.
49 Y. Yuan, C. Brady, L. Annamalai, R. F. Lobo and B. Xu, *J. Catal.*, 2021, **393**, 60–69.
50 N. M. Phadke, J. Van Der Mynsbrugge, E. Mansoor, A. B. Getsoian, M. Head-Gordon and A. T. Bell, *ACS Catal.*, 2018, **8**, 6106–6126.
51 N. M. Phadke, E. Mansoor, M. Bondil, M. Head-Gordon and A. T. Bell, *J. Am. Chem. Soc.*, 2019, **141**, 1614–1627.
52 N. M. Phadke, E. Mansoor, M. Head-Gordon and A. T. Bell, *ACS Catal.*, 2021, 2062–2075.
53 M. W. Schreiber, C. P. Plaisance, M. Baumgärtl, K. Reuter, A. Jentys, R. Bermejo-Deval and J. A. Lercher, *J. Am. Chem. Soc.*, 2018, **140**, 4849–4859.
54 Y. Yuan, C. Brady, R. F. Lobo and B. Xu, *ACS Catal.*, 2021, **11**, 10647–10659.
55 Z. Maeno, S. Yasumura, X. Wu, M. Huang, C. Liu, T. Toyao and K. I. Shimizu, *J. Am. Chem. Soc.*, 2020, **142**, 4820–4832.
56 E. Mansoor, M. Head-Gordon and A. T. Bell, *ACS Catal.*, 2018, **8**, 6146–6162.
57 X. Wang and L. Andrews, *J. Phys. Chem. A*, 2003, **107**, 11371–11379.
58 L. Grocholl, S. A. Cullison, J. Wang, D. C. Swenson and E. G. Gillan, *Inorg. Chem.*, 2002, **41**, 2920–2926.
59 N. Katada, H. Tamagawa and M. Niwa, *Catal. Today*, 2014, **226**, 37–46.
60 E. J. M. Hensen, M. García-Sánchez, N. Rane, P. C. M. M. Magusin, P. H. Liu, K. J. Chao and R. A. Van Santen, *Catal. Lett.*, 2005, **101**, 79–85.
61 A. P. Wilkinson, *Inorg. Chem.*, 1997, **2**, 1602–1607.
62 A. Getsoian, U. Das, J. Camacho-Bunquin, G. Zhang, J. R. Gallagher, B. Hu, S. Cheah, J. A. Schaidle, D. A. Ruddy, J. E. Hensley, T. R. Krause, L. A. Curtiss, J. T. Miller and A. S. Hock, *Catal. Sci. Technol.*, 2016, **6**, 6339–6353.
63 H. Saito and Y. Sekine, *RSC Adv.*, 2020, **10**, 21427–21453.
64 Y. Dai, X. Gao, Q. Wang, X. Wan, C. Zhou and Y. Yang, *Chem. Soc. Rev.*, 2021, **50**, 5590–5630.
65 J. J. H. B. Sattler, J. Ruiz-Martinez, E. Santillan-Jimenez and B. M. Weckhuysen, *Chem. Rev.*, 2014, **114**, 10613–10653.

66 S. De, S. Ould-Chikh, A. Aguilar, J. L. Hazemann, A. Zitolo, A. Ramirez, S. Telalovic and J. Gascon, *ACS Catal.*, 2021, 3988–3995.
67 H. Guo, C. Miao, W. Hua, Y. Yue and Z. Gao, *Microporous Mesoporous Mater.*, 2021, **312**, 110791.
68 H. Seki, H. Saito, K. Toko, Y. Hosono, T. Higo, J. Gil Seo, S. Maeda, K. Hashimoto, S. Ogo and Y. Sekine, *Appl. Catal. A Gen.*, 2019, **581**, 23–30.
69 U. Olsbye, A. Virnovskaia, O. Prytz, S. J. Tinnemans and B. M. Weckhuysen, *Catal. Lett.*, 2005, **103**, 143–148.
70 T. V. M. Rao, E. M. Zahidi and A. Sayari, *J. Mol. Catal. A Chem.*, 2009, **301**, 159–165.
71 A. Tsyganok, R. G. Green, J. B. Giorgi and A. Sayari, *Catal. Commun.*, 2007, **8**, 2186–2193.
72 L. C. Wang, Y. Zhang, J. Xu, W. Diao, S. Karakalos, B. Liu, X. Song, W. Wu, T. He and D. Ding, *Appl. Catal. B Environ.*, 2019, **256**, 117816.
73 Y. He, Y. Song and S. Laursen, *ACS Catal.*, 2019, **9**, 10464–10468.
74 Z. Yang, H. Li, H. Zhou, L. Wang, L. Wang, Q. Zhu, J. Xiao, X. Meng, J. Chen and F. S. Xiao, *J. Am. Chem. Soc.*, 2020, **142**, 16429–16436.
75 Z. Wu, E. C. Wegener, H. T. Tseng, J. R. Gallagher, J. W. Harris, R. E. Diaz, Y. Ren, F. H. Ribeiro and J. T. Miller, *Catal. Sci. Technol.*, 2016, **6**, 6965–6976.
76 E. A. Pidko, V. B. Kazansky, E. J. M. Hensen and R. A. van Santen, *J. Catal.*, 2006, **240**, 73–84.
77 M. S. Pereira and M. A. C. Nascimento, *Chem. Phys. Lett.*, 2005, **406**, 446–451.
78 Z. Fung, X. Liu, Y. Wang, and C. Meng *Molecules*, 2021, **26**, 2234.